Total Structure Characterization of Unsaturated Acidic Phospholipids Provided by Vicinal Di-Hydroxylation of Fatty Acid Double Bonds and Negative Electrospray Ionization Mass Spectrometry

Morten K. Moe, Trude Anderssen, Morten B. Strøm, and Einar Jensen
University of Tromsø, Institute of Pharmacy, Tromsø, Norway

In the present work, the unsaturated fatty acid substituents of some phosphatidic acid, phosphatidylserine, phosphatidylinositol, and phosphatidylglycerol species were converted to their 1,2-di-hydroxy derivatives by OsO_4. The subsequent electrospray ionization tandem low-energy mass spectrometry analysis of the deprotonated species allowed positional determination of the double bonds by the production of specific product-ions. The product-ions are formed by charge-remote and charge-proximate homolytic cleavages as well as charge-directed heterolytic cleavages and rearrangements. The commercial availability of pure species of the phospholipids in question was limited, and a number of species were therefore synthesized. The developed method was used to fully characterize the two isobaric phosphatidylglycerol species 16:0/16:1Δ^9 and 16:0/16:1Δ^{10} extracted from the bacteria *Methylococcus capsulatus*. The presence of these fatty acids was supported by a gas-chromatography mass spectrometry investigation of the dimethyloxazoline derivatives of the species of the lipid extract. The present work demonstrates that a total structure characterization of acidic unsaturated phospholipids in isolate or in mixtures is accomplished by vicinal di-hydroxylation of olefinic sites and subsequent electrospray ionization mass spectrometry of the derivatized phospholipids. (J Am Soc Mass Spectrom 2005, 16, 46–59) © 2004 American Society for Mass Spectrometry

Phospholipids (PLs) are characterized by a glycerol backbone to which a polar phospho-di-ester group is linked at the *sn*-3 carbon, where the alcohol (polar head group) defines the class of the PL. Further, two fatty acids (FAs) are linked at the *sn*-1 and *sn*-2 carbons, respectively, defining the species within the PL class (Figure 1). The structural diversity of PLs is attributable to different polar head groups, FA substituents, and their regioisomerism. These characteristics can be identified by investigating the deprotonated molecules of the PLs by negative electrospray ionization (ESI) tandem quadrupole mass spectrometry (MS) as demonstrated for phosphatidic acid (PA) [1–4], phosphatidylglycerol (PG) [1, 3, 5–7], phosphatidylinositol (PI) [1, 3, 6, 8, 9,], and phosphatidylserine (PS) [1, 3, 4, 8, 10] species. However, a challenging task is to determine the double bond position(s) of unsaturated fatty acids, which are not identified by ESI-MS/MS of the deprotonated native species due to very limited C—C cleavage(s) along the alkenyl chain.

A possible solution is to utilize fast atom bombardment (FAB) in combination with sector mass analyzers for complete structure characterization of PLs [11–13]. Another approach is to convert the double bonds to their ozonide derivatives, as reported by Harrison and Murphy, who identified the double bonds of phosphatidylcholine (PC) species by both positive and negative ESI-MS/MS [14]. The ozonidation reactions were reported to be fast, but incomplete, and some by-products were also formed [14].

However, the addition of OsO_4 to olefins is a selective and reliable organic transformation for two reasons: (1) OsO_4 reacts with virtually all olefins, and (2) it reacts slowly, if at all, with other common organic functional groups [15]. The use of OsO_4 for vicinal di-hydroxylation of double bonds in order to determine olefinic sites in FAs by gas-chromatography (GC)-MS was described in 1965 [16]. Recently, we utilized this strategy in an ESI-MS/MS experiment for determining the positions of double bonds of FAs [17]. The double bonds were converted to their vicinally di-hydroxylated derivatives by treatment with catalytic amounts of OsO_4, and characteristic product-ions unambiguously indicating the hydroxyl group positions were formed upon collisional activated dissociation (CAD) of the deprotonated FAs [17]. We have also reported the

Published online December 9, 2004
Address reprint requests to Dr. M. K. Moe, Institute of Pharmacy, University of Tromsø, N-9037 Tromsø, Norway. E-mail: mortenm@farmasi.uit.no

1044-0305/05/$30.00
doi:10.1016/j.jasms.2004.09.014

Received July 4, 2004
Revised September 13, 2004
Accepted September 14, 2004

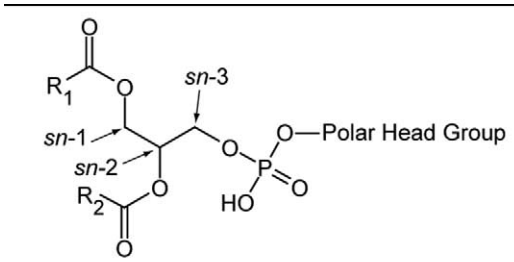

Polar Head Group	Phospholipid	Abbreviation
H	Phosphatidic acid	PA
OH, HO	Phosphatidyl glycerol	PG
HO, HO, OH, OH, OH	Phosphatidyl inositol	PI
COOH, H_2N	Phosphatidyl serine	PS

Figure 1. Structure, glycerol C-atom stereo-specific numbering (*sn*), name, and abbreviations of the acidic phospholipids investigated in the present work. R_1 and R_2 represent alkyl or alkenyl chains.

complete structure characterization of PC and phosphatidylethanolamine (PE) species containing isomeric unsaturated FAs by ESI-MS/MS after treatment with OsO_4 [18].

In the present work, unsaturated FA constituents of PA, PG, PI, and PS species (Figure 1) were derivatized in order to obtain a total structure characterization of acidic PL species by negative ESI-MS/MS. Because of the limited commercial availability of pure and structure-defined species of the PLs in question, synthesis of several PA, PG, and PS species containing an unsaturated FA was conducted in order to ensure structural diversity.

Two bacterial PL species were completely characterized and thereby demonstrated the applicability of the ESI-MS/MS method on real samples. The results of the present work show that vicinal di-hydroxylation of FA constituents of acidic PLs is a powerful strategy for obtaining a complete structure characterization of PLs.

Materials and Methods

Chemicals

The FAs, 2-lysophosphatidylcholine from egg (main constituents: 1-16:0- and 1-18:0-2-lysophosphatidylcholine; ~2:1 wt/wt), serine, glycerol, phospholipase D (*Streptomyces* sp.), ethanol-free chloroform, 2′,7′-dichlorofluorescein, trifluoroacetic acid, Supelclean LC-Si solid phase extraction (SPE) tubes (100 mg; 1 mL), 16:0/18:1Δ^9 PI, 4-aminopyridine (4-APy), dicyclohexylcarbodiimide (DCC), 4-pyrrolidinopyridine (4-PPy), OsO_4 (2.5%; wt/vol, in *tert*-butanol), and 4-methylmorpholine-4-oxide were purchased from Sigma-Aldrich (Steinheim, Germany). Kieselgel 60 (bulk), Kieselgel 60 high performance thin-layer chromatography (HPTLC) plates, 2-amino-2-methylpropanol, $CaCl_2$, $CuSO_4 \cdot H_2O$, ammonium acetate, sodium acetate, acetic acid, and aqueous ammonia (25%) were obtained from Merck (Darmstadt, Germany). Phosphoric acid was purchased from Baker (Dagenham, UK). All solvents had a purity of >99% (except for hexane >95%) and were delivered from Merck or Sigma-Aldrich, except ethanol (96%) from Arcus (Oslo, Norway). The chemicals were purchased in the purest form commercially available. Nitrogen, helium, and argon (>99.99%) were delivered from AGA (Oslo, Norway).

Synthesis of PC [19, 20]

The method used was in accordance with Vodovozova and Molotkovsky [19, 20] with some minor modifications. In brief, 2-lysophosphatidylcholine (5 mg; ~10 μmol) was dried with benzene (1 mL) under reduced pressure. Trifluoroacetic acid (1.5 μL) was added to the dry 2-lysophosphatidylcholine, and excess acid removed under reduced pressure yielding dry 2-lysophosphatidylcholine trifluoroacetate. A suspension of free FA, DCC, 4-APy, and 4-PPy (all: 15 μmol) in dry ethanol-free chloroform (0.3 mL) was added to the dried 2-lysophosphatidylcholine trifluoroacetate in dry ethanol-free chloroform (0.5 mL). The reaction mixture was stirred at r.t. (90 min) and an average yield of >70% PC was obtained according to HPTLC combined with scanning densitometry (see below). The reaction mixture was applied on a glass-wool stoppered column (0.55 mm) containing 1.5 g of Kiselgel 60 in chloroform-methanol (2:1; vol/vol). The column was washed with 5 mL chloroform-methanol-aqueous NH_3 (25%) (60:30:1; vol/vol) and PC was eluted with 10 mL chloroform-methanol-aqueous NH_3 (25%) (50:30:3; vol/vol) [21].

Transesterification of PC [22–24]

PC may undergo either a transesterification with an alcohol forming the desired PL (and liberation of choline) or a hydrolysis to PA and choline in the presence of phospholipase D [25]. Thus, various amounts of PA are always formed given that an aqueous buffer is involved in the reaction. PC (1 mg) dissolved in diethyl ether (1 mL) was added to 0.5 mL 100 mM aqueous sodium acetate/acetic acid buffer (pH 5.6) also containing 40 mM $CaCl_2$, 5 units of phospholipase D, and glycerol or serine. The concentration in the aqueous solution was 2% (vol/vol) for

glycerol and 20% (wt/vol) for serine. The incubation was carried out by stirring for 3 h at 30 °C to ensure complete mixing of both phases. Subsequently, the vials were left to rest for 5 minutes to ensure complete phase separation. The ether phase was transferred into a second vial and the aqueous phase was extracted once with 1 mL diethyl ether. The ether phases were combined and evaporated under a stream of nitrogen. PC was totally converted to either the transphosphatidylation products PG or PS, or to the hydrolyzed product PA. The yield was >90% for PG and ~50% for PS as judged by HPTLC.

Preparation of Vicinally Di-Hydroxylated FA Components of PLs

The procedure for vicinal di-hydroxylation is described in a previous paper [17] and references therein. In brief, 0.1–0.5 mg PL was added to 2 mL 4-methylmorpholine-4-oxide (2%; wt/vol) in methanol-chloroform-water (2:1:0.1; vol/vol) containing 5 μL OsO_4 solution (catalyst). The reaction proceeded at r.t. for 3 h under N_2.

Extraction of Lipids from Methylococcus capsulatus [26–28]

To 200 mg freeze-dried bacteria in a test tube, 2 × 2 mL chloroform and 1 × 2 mL methanol were added portion-wise followed by sonication (30 min) after each addition. The mixture was transferred to a 25 mL separation funnel with 3 × 2 mL of chloroform-methanol (2:1; vol/vol). 2 mL water was then added and the funnel was shaken for 1 min and allowed to rest for 18 h. The organic layer was carefully drained off and the solvents removed under a stream of nitrogen at 45 °C overnight to ensure a total removal of water. A lipid content of 10.4 ± 0.2% (four aliquots) was determined by gravimetry [27].

HPTLC

Developing mixtures of either chloroform-ethanol-triethylamine-water (30:34:30:8; vol/vol) [29]; retention factors (R_f): 0.14 (PC); 0.20 (PS); 0.26 (PA); and 0.56 (PG), or chloroform-acetone-methanol-acetic acid-water (5:2:1:1:0.5, vol/vol) [30], R_f: 0.24 (2-lysophosphatidylcholine) and 0.47 (PC), were used. The bands were visualized by either (1) carefully spraying the plate with 0.2% ethanolic 2′,7′-dichlorofluorescein in which the bands appeared as fluorescent spots (UV 366 nm; non-destructive) [31], or by (2) dipping the plate in an aqueous $CuSO_4$ (10%; wt/vol) and H_3PO_4 (8%; vol/vol) solution with subsequent heating at 180 °C for 20 min (destructive).

Scanning Densitometry

Scanning densitometry was performed on a TLC Scanner 3 from CAMAG (Muttentz, Switzerland) operating at 530 nm controlled by the CATS v. 4.06 software.

Dimethyl-Oxazoline (DMOX) Preparation [32, 33]

The FA constituents of the extracted lipids were converted to their DMOX derivatives by adding 250 μL 2-amino-2-methylpropanol to 10 mg of the extract and heating the mixture at 180 °C for 18 h. After cooling to r.t., the mixture containing the DMOX derivates was diluted with 5 mL CH_2Cl_2. Excess 2-amino-2-methylpropanol was removed by washing with 2 × 2 mL water and the CH_2Cl_2 was removed under a stream of nitrogen at 40 °C. The hexane (1 mL) redissolved DMOX derivatives were applied on a hexane-conditioned 100 mg LC-Si SPE column and eluted by 4 mL hexane-EtOAc (9:1 vol/vol). Finally, the solvent was removed under a stream of nitrogen at r.t., and the DMOX derivatives were redissolved in hexane.

GC-MS of DMOX Derivatives

A GC 8000 connected to a MD 800 quadrupole mass analyzer (Fisons, Milan, Italy) equipped with a 60 m CP-Sil 5 CB low bleed MS column (i.d. = 0.25 mm) from Chrompack (Bergen op Zoom, The Netherlands) was used for this purpose. Helium (flow 1.2 mL min^{-1}) was used as carrier gas, the injector temperature was 220 °C and 1 μL sample (splitless 30 s) was injected. The oven temperature program was initially 40 °C (3 min) then increased with 30 °C min^{-1} to 140 °C (3 min), and finally 3 °C min^{-1} to 270 °C (32 min). The mass spectrometer interface and the electron ionization (EI) source temperatures were 265 °C and 200 °C, respectively. The EI energy was 70 eV.

ESI-MS/MS

The mass spectrometer was a tandem quadrupole QuattroLC from Micromass (Manchester, UK) controlled by MassLynx 3.4 software. The MS instrument was further equipped with a syringe pump (Harvard Apparatus, Holliston, MA), and a 250 μL syringe (SGE, Ringwood, Victoria, Australia). The PLs were infused into the mass spectrometer at 10 μL min^{-1}. The desolvation and cone gas flows (N_2) were 125 L h^{-1} and 30 L h^{-1}, respectively, the capillary and cone voltages were 3.2 kV and 70 V, respectively, and the laboratory frame energy (E_{Lab}) was applied as indicated throughout the text. The collision gas (argon) pressure was $1{\cdot}10^{-3}$ Pa ($7.5{\cdot}10^{-6}$ torr). The desolvation and the source temperatures were 120 and 90 °C, respectively.

Nomenclature

The PL species of the present work are abbreviated as follows, e.g., 16:0/18:1Δ^9 PS corresponds to 1-hexadecanoyl-2-(9)-octadecenoyl-*sn*-glycero-phosphoserine (IUPAC nomenclature). The FA abbreviation is "number of carbon atoms:number of double bonds$\Delta^{\text{position(s) of double bond(s)}}$", e.g., 18:1$\Delta^9$. The derivatized FAs are abbreviated as 9,10-$(OH)_2$-18:0, i.e., 9,10-dihydroxy-octadecanoic acid. All the unsaturated FAs investigated in the present work were *cis*-configured. The ion nomenclature used is in accordance with Hsu and Turk [2, 7, 9], except for the neutral loss of the polar head group (Y) from PG, PI, and PS which are abbreviated G (i.e., prop-2-ene-1,2-diol, 74 u), I (i.e., [inositol − H_2O], 162 u), and S (i.e., 2-amino-propenoic acid, 87 u), respectively.

Results

Structure Characterization of PLs in General

In accordance with previous reports, all the PL species investigated in the present study produced abundant $[M - H]^-$ ions upon ESI [1–10]. Fragmentation reactions involving heteroatoms are favored because of the lower critical energy of such reactions and this applies especially to the low-energy regime of tandem quadrupole MS. CAD analysis of deprotonated PLs represents no exception to this principle.

Given that R_x is the *sn*-1 (R_1) and the *sn*-2 (R_2) FA of the PL, respectively, the following series of five different product-ions were produced upon CAD of the $[M - H]^-$: (1) neutral loss of a FA, i.e., $[M - H - R_xCOOH]^-$; (2) neutral loss of a ketene, i.e., $[M - H - R'_xCH{=}C{=}O]^-$; (3) neutral loss of the polar head group (Y) and a fatty acid, i.e., $[M - H - Y - R_xCOOH]^-$; (4) neutral loss of the polar head group and a ketene, i.e., $[M - H - Y - R'_xCH{=}C{=}O]^-$; and (5) formation of carboxylate anions, i.e., R_xCOO^- [1–10]. Deprotonated PA, PG, PI, and PS species all show a preferred loss of the *sn*-2 FA either as a neutral FA or as a neutral ketene (product-ions 1–4) upon CAD [1–10], which are useful for assigning FA regioisomerism. Regarding the R_xCOO^- ions (5), the ion abundance ratio R_2/R_1 is >1 for PG and <1 for PA and PS, which is useful for regioisomeric determination, whereas for PI this ratio fluctuates around one [1–10]. The ions at *m/z* 153 $[H_2C{=}C(OH)CH_2\text{-}PO_4H]^-$, *m/z* 97 $[H_2PO_4]^-$, and *m/z* 79 $[PO_3]^-$ were observed in the CAD product-ion spectra of all PLs.

In the following section, a brief summary of the observed product-ions from native deprotonated PA, PG, PI, and PS species is presented, but no information about double bond positions can be obtained from these spectra. The CAD product-ion spectra of the derivatized PLs are also presented and these show product-ions indicative for the position of the hydroxyl groups. The deprotonated molecule $[M - H]^-$ is the precursor for the formation of all product-ions discussed.

16:0/18:1Δ^{11}PA

Figure 2a shows the product-ion spectrum of $[M - H]^-$ of 16:0/18:1Δ^{11} PA, *m/z* 673, recorded at E_{Lab} 30 eV. The product-ions $[M - H - R_1COOH]^-$, $[M - H - R_2COOH]^-$, $[M - H - R'_1CH{=}C{=}O]^-$, and $[M - H - R'_2CH{=}C{=}O]^-$ are observed at *m/z* 417, 391, 435, and 409, respectively. Additionally, R_1COO^- and R_2COO^- are observed at *m/z* 255 (100%) and 281 (53%) respectively. These ions and their abundances are in accordance with previous reports [1–4]. A mechanism for the formation of R_2COO^- is shown in Scheme **1** (upper part) [2, 4, 7] which applies to all PL species constituting both native and derivatized FAs.

It is reported that CAD product-ion spectra of free FAs provide information about double bond positions [34]. However, an increment to E_{Lab} 60 eV did not provide information about the double bond position of the 18:1Δ^{11} carboxylate, as demonstrated in the CAD product-ion spectrum of 16:0/18:1Δ^{11} PA (Figure 2b).

16:0/11,12-$(OH)_2$-18:0 PA

Figure 2c and d show the product-ion spectra of $[M - H]^-$ of 16:0/11,12-$(OH)_2$-18:0 PA, *m/z* 707, recorded at E_{Lab} 30 and 60 eV, respectively. The spectrum obtained at E_{Lab} 30 eV (Figure 2c) resembles the spectrum of the native compound (Figure 2a); but the ions $[M - H - R'_1CH{=}C{=}O]^-$, at *m/z* 469, $[M - H - R_1COOH]^-$, at *m/z* 451, and R_2COO^-, at *m/z* 315, are all shifted by 34 u. The ion-intensity ratios $[M - H - R'_2CH{=}C{=}O]^-/[M - H - R'_1CH{=}C{=}O]^-$ and R_2COO^-/R_1COO^- are comparable to those of the native species and their hydroxylated analogues when recorded at E_{Lab} 30 eV. The ratio of the ions $[M - H - R_2COOH]^-/[M - H - R_1COOH]^-$, however, was found to fluctuate around one for the hydroxylated species investigated in the present work (n = 7) and is thus not useful for regioisomeric determination. However, the applied laboratory frame energy is too low to induce fragmentations along the alkyl chain of the hydroxylated R_2 carboxylate.

The E_{Lab} 60 eV CAD product-ion spectrum (Figure 2d) deviates from the other spectra as it contains no peaks above *m/z* 315, which corresponds to deprotonated 11,12-$(OH)_2$-18:0. In addition, ions determining the position of the two hydroxyl groups are observed. These ions are results of C—C cleavages adjacent to the hydroxyl groups, as outlined in Scheme **1** (lower part) [35]. The ions at *m/z* 229 and 199 are presumably formed by homolytic cleavage of the C13—C12 and the C12—C11 bond with subsequent loss of a hydrogen radical (Scheme **1a** and **1b**, respectively), with the charge retained at the carboxylate group. The ions at *m/z* 143 and 113 are formed by a charge-migration from the carboxylate group to the C12—oxygen (Scheme **1c1** and **d1**) followed by cleavage of the C11—C10 and the C12—C11 bond (Scheme **1c2** and **1d2**, respectively). As no ions indi-

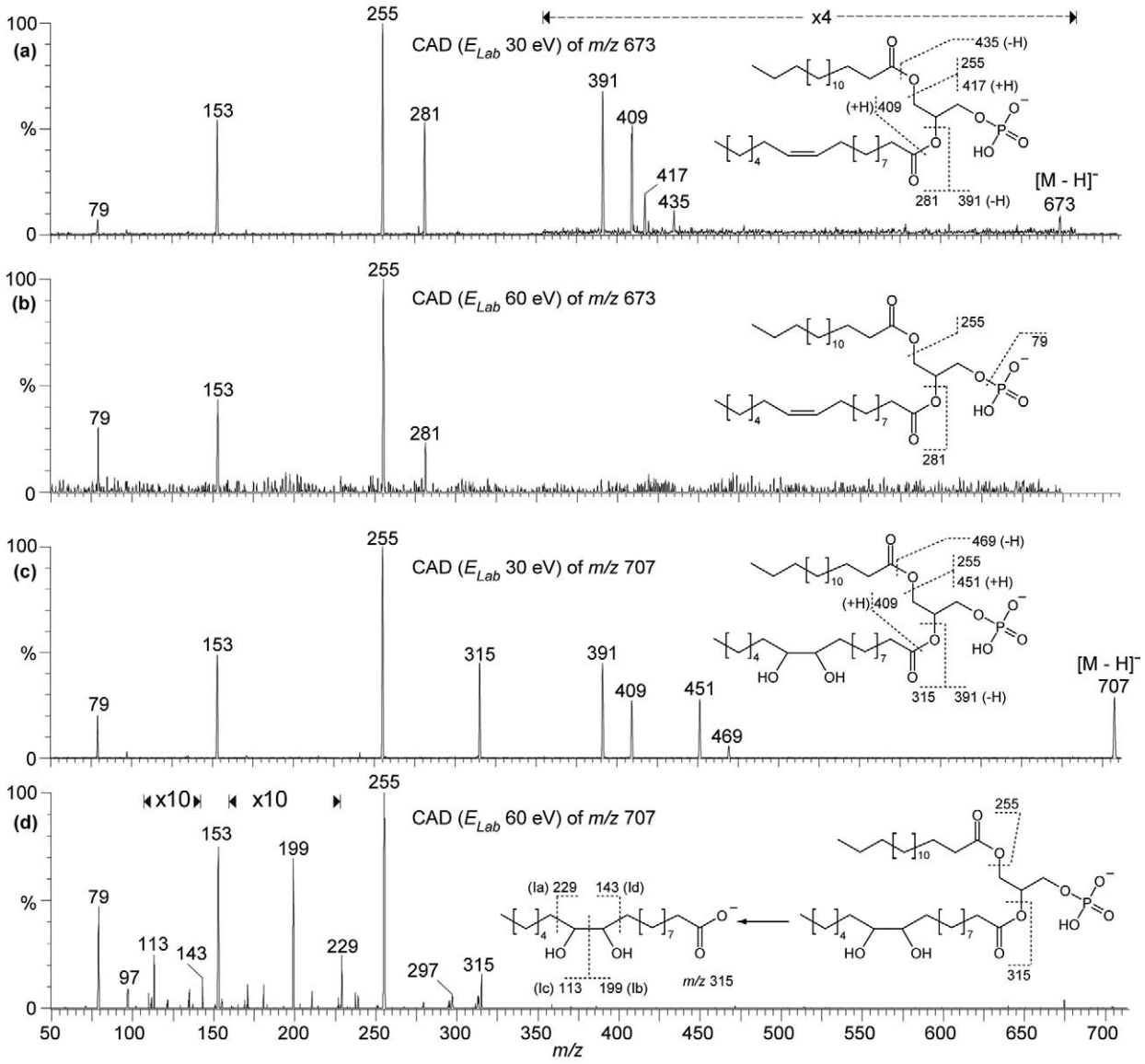

Figure 2. Product-ion spectra of deprotonated (**a**) and (**b**) 16:0/18:1Δ^{11} PA, *m/z* 673, recorded at E_{Lab} 30 and 60 eV, respectively; (**c**) and (**d**) 16:0/11,12-$(OH)_2$-18:0 PA, *m/z* 707, recorded at E_{Lab} 30 and 60 eV, respectively. In (**d**), *m/z* of structurally important ions are shown on the structure and these ions are formed by the mechanism indicated in parenthesis.

cating the hydroxyl groups are observed above *m/z* 315, it is suggestive that the ester bond is cleaved prior to further fragmentation of the derivatized FA. This is possible as multiple collisions are expected to occur in the quadrupole collision cell. A summary of the *m/z* values of ions formed by the mechanisms **1a–1d** (Scheme **1**) from the present derivatized FAs is given in Table 1.

16:0/18:1Δ^9 PI

The CAD product-ion spectrum of deprotonated 16:0/18:1Δ^9 PI, *m/z* 835 recorded at E_{Lab} 30 eV, is shown in Figure 3a. A more thoroughly discussion of ESI-MS/MS of native deprotonated PI species are given elsewhere [1, 3, 6, 8, 9]. However, the origin of some important product-ions is shown in Figure 3a.

16:0/9,10-$(OH)_2$-18:0 PI

The CAD product-ion spectrum of deprotonated 16:0/9,10-$(OH)_2$-18:0 PI, *m/z* 869, recorded at E_{Lab} 65 eV, is shown in Figure 3b. The R_1COO^- and R_2COO^- ions appear at *m/z* 255 and 315, respectively. From the latter, the ions indicating C10—OH at *m/z* 201 and 141 are formed by mechanisms **1a** and **1c** (Scheme **1**), whereas the ion indicating C9—OH at *m/z* 171 is produced by mechanisms **1b** and **1d**. The ion at *m/z* 125 is probably formed by mechanism **2b** in Scheme **2** (x = 0) with additional loss of H_2.

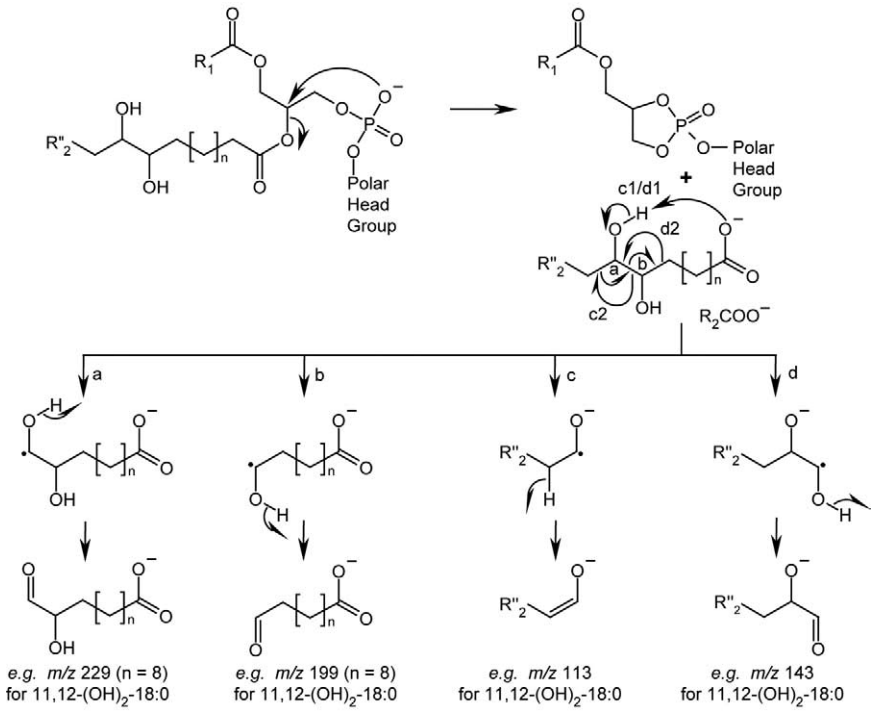

Scheme 1. (Upper part) A charge-directed mechanism for the formation of R_2COO^- [2, 4, 7]. (Lower part) Proposed mechanisms for the formation of (**a**) *m/z* 229, (**b**) *m/z* 199, (**c**) *m/z* 113, and (**d**) *m/z* 143 from deprotonated 11,12-$(OH)_2$-18:0 [35].

16:0/18:1Δ^6 PS [1, 3, 4, 8, 10]

The CAD product-ion spectrum of deprotonated 16:0/18:1Δ^6 PS, *m/z* 760, recorded at E_{Lab} 30 eV, is shown in Figure 4a. An abundant ion at *m/z* 673, $[M - H - S]^-$, is formed due to loss of a neutral 2-aminopropenoic acid (S; 87 u) from $[M - H]^-$. The ions at *m/z* 391, 417, 409, and 435 correspond to $[M - H - S - R_2COOH]^-$, $[M - H - S - R_1COOH]^-$, $[M - H - S - R'_2CH{=}C{=}O]^-$, and $[M - H - S - R'_1CH{=}C{=}O]^-$, respectively. The R_1COO^- and R_2COO^- ions are observed at *m/z* 281 (58%) and 255 (100%), respectively.

16:0/6,7-$(OH)_2$-18:0 PS

The CAD product-ion spectrum of deprotonated 16:0/6,7-$(OH)_2$-18:0 PS, *m/z* 794, recorded at E_{Lab} 60 eV is displayed in Figure 4b. Deprotonated 6,7-$(OH)_2$-18:0, *m/z* 315, undergoes several additional fragmentation reactions and the ions at *m/z* 213 (low abundance) and 183 are formed by the reactions **1c** and **1d** in Scheme **1**, respectively. The transient ions at *m/z* 159 and 129 are formed by mechanisms **1a** and **1b** (Scheme **1**) and loss of CO_2 from these ions by mechanism **2b2** (Scheme **2**) results in the ions at *m/z* 115 and 85, indicating C7—OH and C6—OH, respectively.

16:0/18:2Δ^{9,12} PS

The product-ion spectrum of deprotonated 16:0/18:2Δ^{9,12} PS, *m/z* 758, recorded at E_{Lab} 30 eV is shown in Figure 5a. The formation of the most abundant ions are discussed above and their *m/z* values are shown in Figure 5a [1, 3, 4, 8, 10].

Table 1. *m/z* values of the product-ions formed by the pathways proposed in Scheme 1 for the FA constituents of the PL species investigated in the present work

	Pathway			
Fatty acid	1a	1b	1c	1d
6,7-$(OH)_2$-18:0	(159) → 115[a]	(129) → 85[a]	183	213
9,10-$(OH)_2$-18:0	201	171	141	171
11,12-$(OH)_2$-18:0	229	199	113	143
15,16-$(OH)_2$-18:0	285	255	57	87
9,10,12,13-$(OH)_4$-18:0	201	171	99	129
6,7,9,10,11,12-$(OH)_6$-18:0	159	129	99	129
9,10,12,13,15,16-$(OH)_6$-18:0	201	171	57	87

[a]Ion produced by further loss of and CO_2 by pathway 2b2, Scheme **2.**

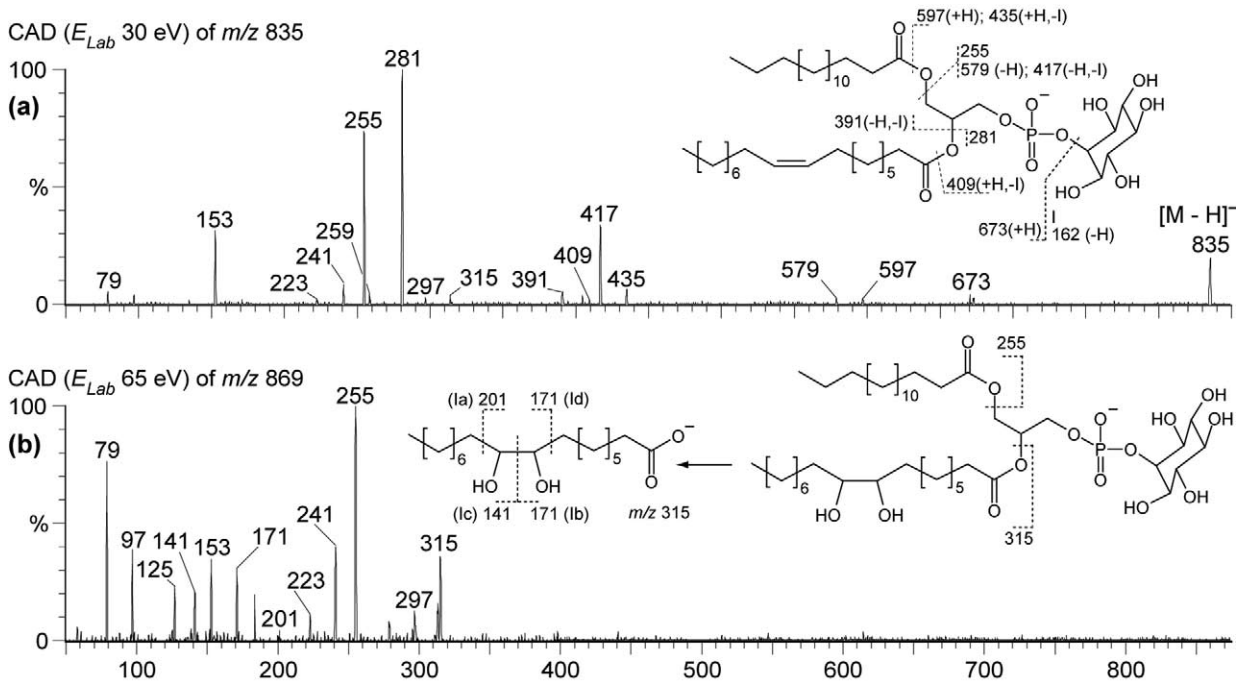

Figure 3. Product-ion spectra of deprotonated (**a**) 16:0/18:1Δ^9 PI, *m/z* 835; E_{Lab} 30 eV, and (**b**) 16:0/9,10-$(OH)_2$-18:0 PI, *m/z* 869; E_{Lab} 60 eV. The ions at *m/z* 259, 241, and 223 are PI specific. In (**b**), *m/z* of structurally important ions are shown on the structure and these ions are formed by the mechanism indicated in parenthesis.

16:0/9,10,12,13-$(OH)_4$-18:0 PS

The product-ion spectrum of deprotonated 16:0/9,10,12,13-$(OH)_4$-18:0 PS, *m/z* 826, recorded at E_{Lab} 65 eV, is shown in Figure 5b. The base peak is R_1COO^- at *m/z* 255, and except for the ions at *m/z* 79, 97, and 153, the remaining ions are formed by cleavages adjacent to the hydroxyl groups in the 9,10,12,13-$(OH)_4$-18:0 carboxylate at *m/z* 347. The ions at *m/z* 171, 129, and 99 are

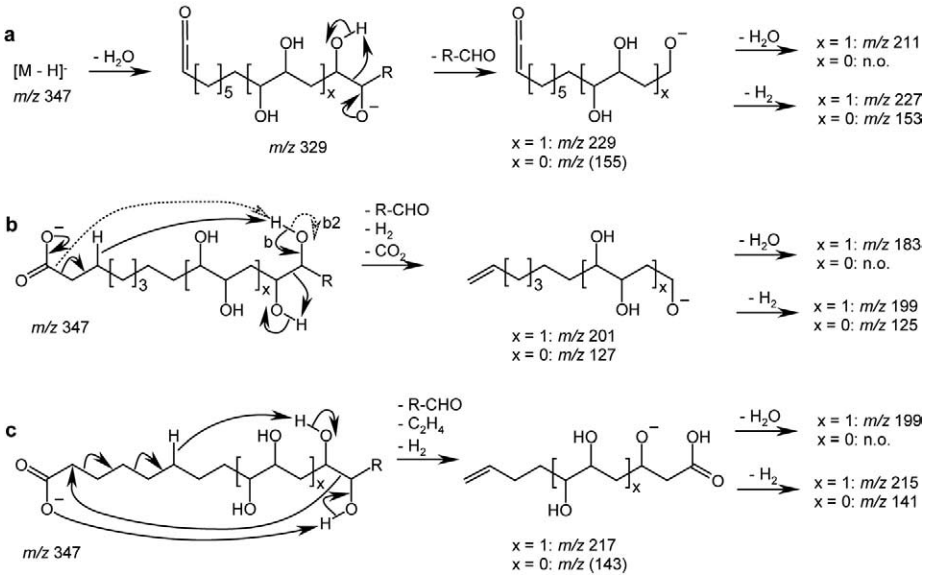

Scheme 2. (**a**)–(**c**) Charge-driven fragmentation mechanisms proposed to operate in vicinally hydroxylated FA carboxylates using 9,10,12,13-$(OH)_4$-18:0 as an example. (**b**) A special case is observed for 6,7-$(OH)_2$-18:0 where CO_2 seems to be lost from the ions produced by Pathways 1a and 1b (Scheme **1**). A mechanism for this loss is proposed by mechanism 2b2 (x = 0), which shows proton abstraction from C7—OH. This abstraction may also occur from C6—OH as well. Note that when x = 0, loss of water is not possible from the ion produced by the proposed mechanisms (**a**)–(**c**).

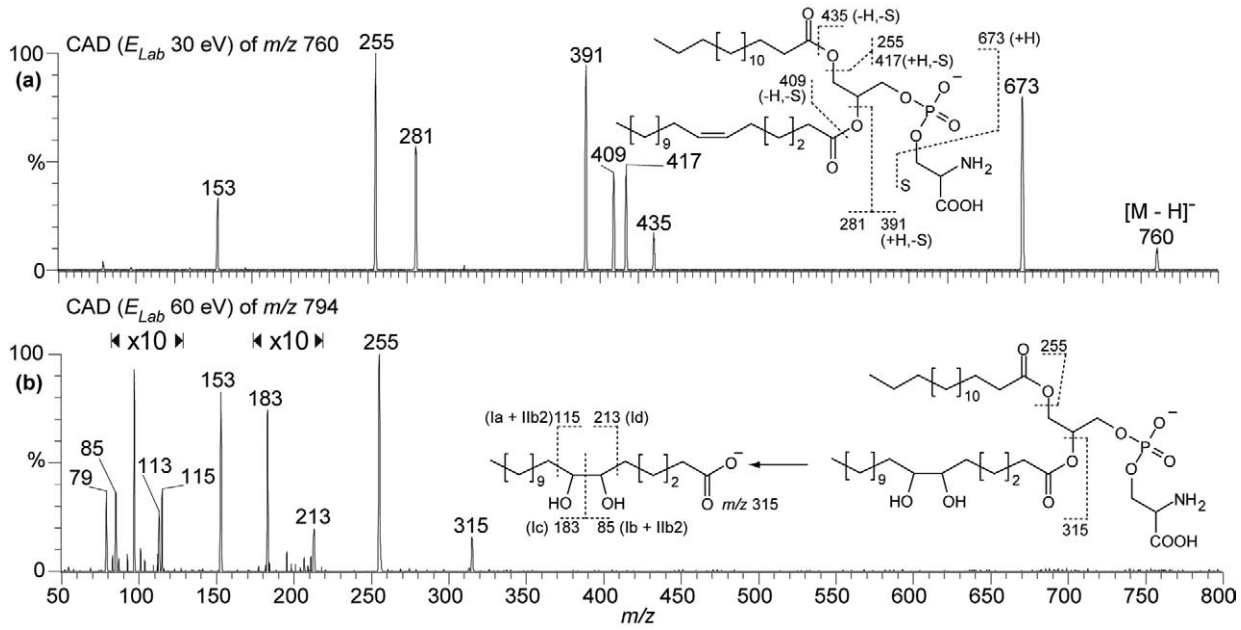

Figure 4. Product-ion spectra of deprotonated (**a**) 16:0/18:1Δ^6 PS, *m/z* 760; E_{Lab} 30 eV, and (**b**) 16:0/6,7-$(OH)_2$-18:0 PS, *m/z* 794; E_{Lab} 60 eV. In (**b**), *m/z* of structurally important ions are shown on the structure and these ions are formed by the mechanism indicated in parenthesis.

formed by mechanisms **1b**–**1d** (Scheme **1**). The ion at *m/z* 201 is more abundant in Figure 5e than it is in Figure 3e (and Figure 6f). This suggests that the ion is formed by more than one mechanism. Scheme **2** displays three charge-directed mechanisms proposed to operate in 9,10,12,13-$(OH)_4$-18:0 derived from our previous work [35]. Mechanism **2b** shows that the ion at *m/z* 201 also is formed by this mechanism. The same

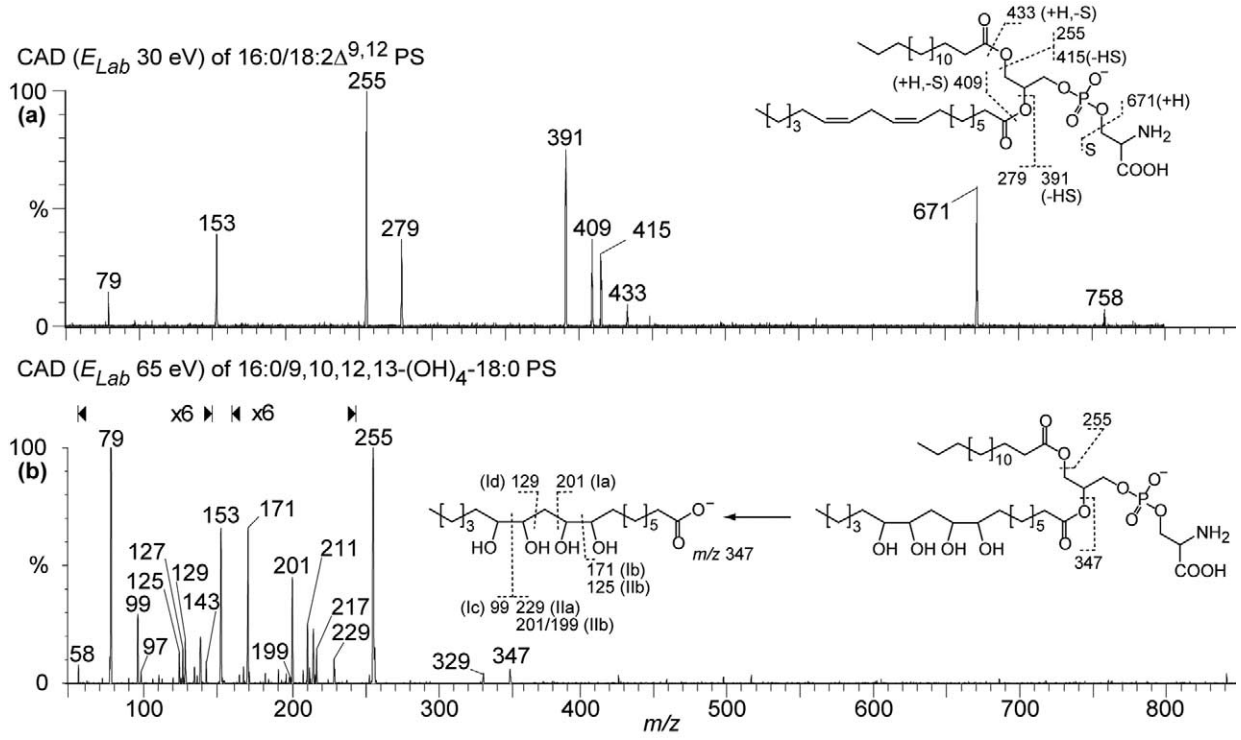

Figure 5. Product-ion spectra of deprotonated (**a**) 16:0/18:2$\Delta^{9,12}$ PS, *m/z* 758; E_{Lab} 30 eV, and (**b**) 16:0/9,10,12,13-$(OH)_4$-18:0, *m/z* 826; E_{Lab} 60 eV. In (**b**), *m/z* of structurally important ions are shown on the structure and these ions are formed by the mechanism indicated in parenthesis.

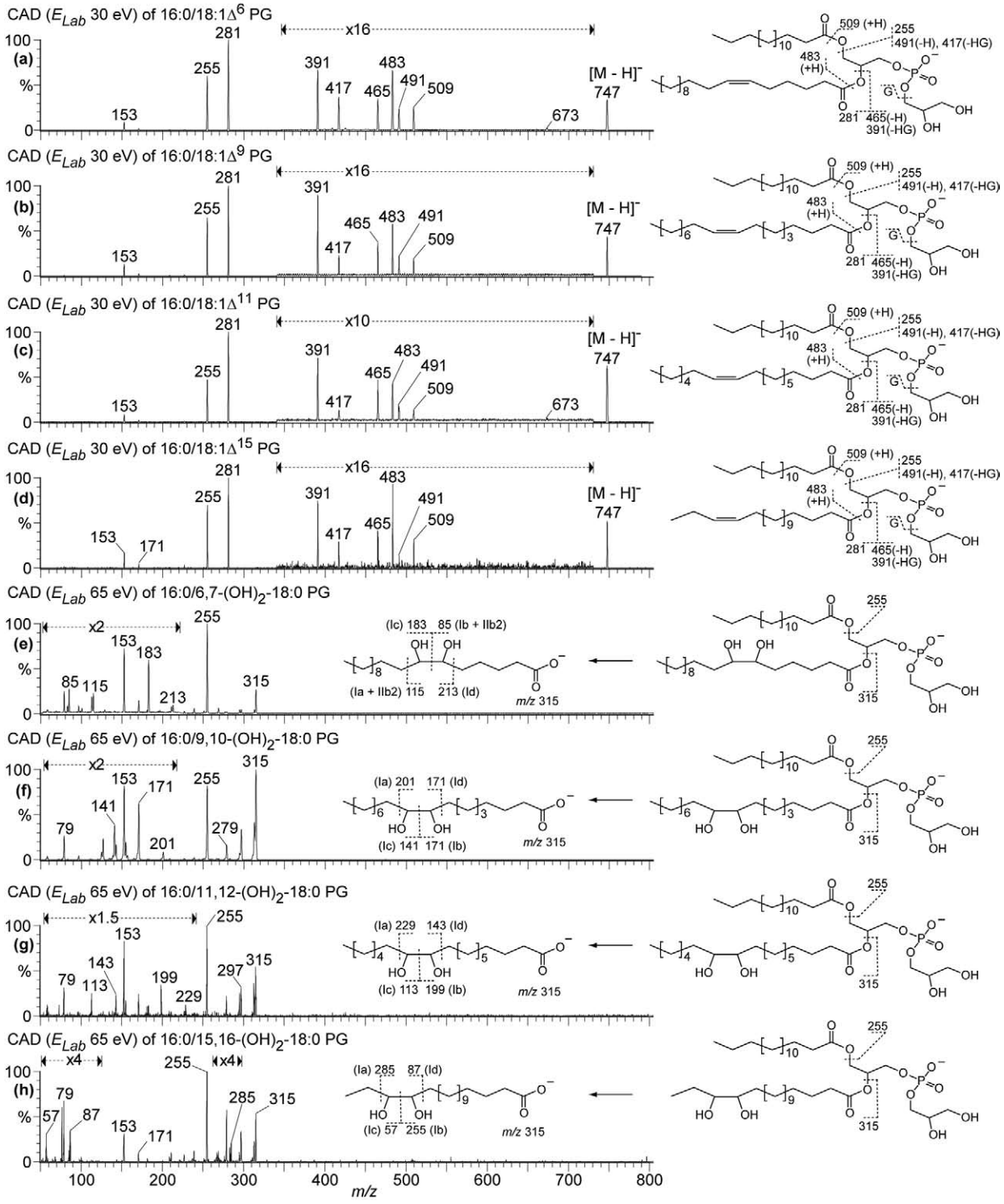

Figure 6. The product-ion spectra of the deprotonated PG species (**a**) 16:0/18:1Δ^6, (**b**) 16:0/18:1Δ^9, (**c**) 16:0/18:1Δ^{11}, and (**d**) 16:0/18:1Δ^{15}, all *m/z* 747, and (**e**) 16:0/6,7-$(OH)_2$-18:0, (f) 16:0/9,10-$(OH)_2$-18:0, (**g**) 16:0/11,12-$(OH)_2$-18:0, and (**h**) 16:0/15,16-$(OH)_2$-18:0, all *m/z* 781. E_{Lab} 30 eV; (**a**)–(**d**), 65 eV; (**e**)–(**h**). In (**e**)–(**h**), *m/z* of structurally important ions are shown on the structures and these ions are formed by the mechanism indicated in parenthesis.

mechanism also accounts for the ion at *m/z* 125. Mechanism **2a** yields the ions at *m/z* 229 and 153, the latter overlaps with the $[H_2C{=}C(OH)CH_2\text{-}PO_4H]^-$ ion. The rearrangement reaction (**2c**) accounts for the ions at *m/z* 217 and 143. A summary of the ions produced by the mechanisms **2a**–**2c** is given in Table 2. Included in this

Table 2. *m/z* values of the product-ions formed by the pathways proposed in Scheme 2 for FA constituents containing four or more hydroxyl groups

			Pathway 2a			Pathway 2b			Pathway 2c		
Fatty Acid	x	R	*m/z*	loss	*m/z*	*m/z*	loss	*m/z*	*m/z*	loss	*m/z*
9,10,12,13-$(OH)_4$-18:0	1	C_5H_{11}	229	$\xrightarrow{H_2}$	(227)	201	$\xrightarrow{H_2}$	199	217	$\xrightarrow{H_2}$	215
	1	C_5H_{11}	229	$\xrightarrow{H_2O}$	211	201	$\xrightarrow{H_2O}$	183[w]	217	$\xrightarrow{H_2O}$	199
	0	$C_8H_{17}O_2$	155[w]	$\xrightarrow{H_2}$	153[a]	127	$\xrightarrow{H_2}$	125	143	$\xrightarrow{H_2}$	(141)
	0	$C_8H_{17}O_2$	155[w]	$\xrightarrow{H_2O}$	n.o.	127	$\xrightarrow{H_2O}$	n.o.	143	$\xrightarrow{H_2O}$	n.o.
6,7,9,10,12,13-$(OH)_6$-18:0	2	C_5H_{11}	(261)*	$\xrightarrow{H_2}$	(259)*	(233)	$\xrightarrow{H_2}$	231	249[w]	$\xrightarrow{H_2}$	(247)
	2	C_5H_{11}	(261)*	$\xrightarrow{H_2O}$	(243)*	(233)	$\xrightarrow{H_2O}$	215[w]	249[w]	$\xrightarrow{H_2O}$	231
	1	$C_8H_{17}O_2$	187	$\xrightarrow{H_2}$	(185)	159	$\xrightarrow{H_2}$	157[w]	175[w]	$\xrightarrow{H_2}$	173
	1	$C_8H_{17}O_2$	187	$\xrightarrow{H_2O}$	169	159	$\xrightarrow{H_2O}$	141	175[w]	$\xrightarrow{H_2O}$	157[w]
	0	$C_{11}H_{23}O_4$	113	$\xrightarrow{H_2}$	111	85[w]	$\xrightarrow{H_2}$	83	101[w]	$\xrightarrow{H_2}$	99
	0	$C_{11}H_{23}O_4$	113	$\xrightarrow{H_2O}$	n.o.	85[w]	$\xrightarrow{H_2O}$	n.o.	101[w]	$\xrightarrow{H_2O}$	n.o.
9,10,12,13,15,16-$(OH)_6$-18:0	2	C_2H_5	(303)*	$\xrightarrow{H_2}$	(301)*	(275)	$\xrightarrow{H_2}$	273	291[w]	$\xrightarrow{H_2}$	(289)
	2	C_2H_5	(303)*	$\xrightarrow{H_2O}$	285[w]	(275)	$\xrightarrow{H_2O}$	257[w]	291[w]	$\xrightarrow{H_2O}$	273
	1	$C_5H_{11}O_2$	229	$\xrightarrow{H_2}$	227[w]	201	$\xrightarrow{H_2}$	199	217	$\xrightarrow{H_2}$	215
	1	$C_5H_{11}O_2$	229	$\xrightarrow{H_2O}$	211	201	$\xrightarrow{H_2O}$	183[w]	217	$\xrightarrow{H_2O}$	199
	0	$C_8H_{17}O_4$	155	$\xrightarrow{H_2}$	153[a]	127	$\xrightarrow{H_2}$	125	143[w]	$\xrightarrow{H_2}$	141[w]
	0	$C_8H_{17}O_4$	155	$\xrightarrow{H_2O}$	n.o.	127	$\xrightarrow{H_2O}$	n.o.	143[w]	$\xrightarrow{H_2O}$	n.o.

The letters x and R correspond to the letter associated with the bracket and the rest-group in Scheme **2**, respectively. The product-ions are prone to undergo loss of H_2 or (and) H_2O, and *m/z* values for these additional reactions are also included in the table.
*The ion is observed in the CAD product ion of $[M-H]^-$ of the free hydroxylated FA
[w]Low abundant ion
[a]The ion is overlapping with the $[H_2C=C(OH)CH_2\text{-}PO_4H]^-$ ion. Ions in brackets are not observed.

table are the *m/z* values for ions resulting from further loss of H_2 or water from some of the end products of mechanisms **2a–2c**. When any of the mechanisms **2a–2c** operate on the proximal pair of OH-groups (x = 0), loss of water is not observed from the end products.

16:0/18:1Δ^n PG

The product-ion spectra of the deprotonated PG species 16:0/18:1Δ^6, 16:0/18:1Δ^9,16:0/18:1Δ^{11},and 16:0/18:1Δ^{15}, recorded at E_{Lab} 30 eV, are almost identical as shown in Figure 6a–d, respectively. Details on the origin of the product-ions are given in the figures and these are in accordance with previous reports [1, 3, 5–7].

16:0/n,n+1-$(OH)_2$-18:0 PG

The product-ion spectra recorded at E_{Lab} 65 eV of the vicinally di-hydroxylated derivatives of the PG species in Figure 6a–d are shown in Figure 6e–h. The R_1COO^- ion is observed at *m/z* 255 whereas the R_2COO^- ion is observed at *m/z* 315. The latter ion undergoes further fragmentations and a summary of the product-ions formed that are indicative for the positions of the hydroxyl groups is displayed in Table 1 and shown in Figure 6e–h. These ions are all formed according to the mechanisms **1a–1d** outlined in Scheme **1**. The spectra in Figure 6e–h show that isobaric PL species containing different isomeric FAs are easily distinguished by the present method.

16:0/6,7,9,10,12,13-$(OH)_6$-18:0 and 16:0/9,10,12,13,15,16-$(OH)_6$-18:0 PG

Isobaric deprotonated isomeric PG species produce almost identical CAD product-ion spectra as demonstrated in Figure 6a–d. This is also the case for deprotonated 16:0/18:3Δ^{6,9,12} PG and 16:0/18:3Δ^{9,12,15} PG, and their CAD product-ion spectra are thus not shown. The CAD product-ion spectra of deprotonated 16:0/6,7,9,10,12,13-$(OH)_6$-18:0 PG and 16:0/9,10,12,13,15,16-$(OH)_6$-18:0 PG, both *m/z* 845 (E_{Lab} 65 eV) are displayed in Figure 7a and b, respectively. The R_1COO^- and R_2COO^- ions are observed at *m/z* 255 and *m/z* 379, respectively, in both spectra.

In Figure 7a, the 6- and 7-hydroxyl groups are identified by the *m/z* 129 (and *m/z* 83) and the *m/z* 159 (and *m/z* 113) ions, respectively, as discussed for 16:0/6,7-$(OH)_2$-18:0 PS above. Several ions formed by the pathways drawn in Scheme **2** are observed that allow the identification of the six hydroxyl groups and a

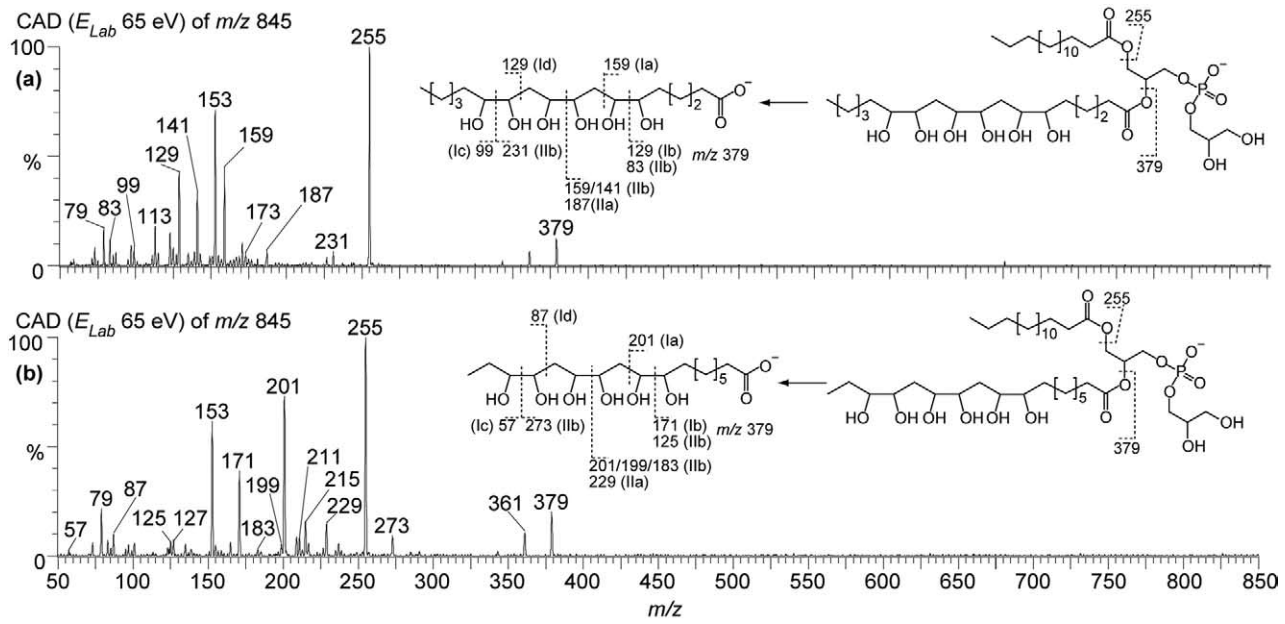

Figure 7. The product-ion spectra (E_{Lab} 65 eV) of $[M - H]^-$ (*m/z* 845) of (**a**) 16:0/6,7,9,10,12,13-$(OH)_6$-18:0 PG and (**b**) 16:0/9,10,12,13,15,16-$(OH)_6$-18:0 PG. In both (**a**) and (**b**), *m/z* of structurally important ions are shown on the structures and these ions are formed by the mechanism indicated in parenthesis.

summary of these ions is given in Table 2. The ions at *m/z* 159 and 129 are more abundant in Figure 7a than in Figure 5b, since more than one reaction pathway may result in these ions. The ion indicating C12—OH at *m/z* 129 is formed by Pathway **1d** (Scheme **1**), and *m/z* 159 is formed by Pathway **2b** (Scheme **2** and Table 2). The C13—OH is identified by the *m/z* 99 ion, formed by Pathway **1c**. It should be emphasized that the charge-directed mechanisms in Scheme **2** tend to dominate over the charge-remote reactions (Scheme **1**) with increasing number of hydroxyl groups.

From the deprotonated 9,10,12,13,15,16-$(OH)_6$-18:0, ions formed by Pathway **1a**–**1d** (Scheme **1**) are observed at *m/z* 201, 171, 57, and 87, respectively. The remaining identified structure characterstic ions are formed by the charge-directed mechanisms in Scheme **2** and a summary of these ions is found in Table 2. Thus, the production of the different fragment ions from the 6,7,9,10,12,13- and 9,10,12,13,15,16-$(OH)_6$-18:0 anions allows for the distinction among these two PG isomers.

Characterization of Phospholipids from Methylococcus capsulatus

In order to investigate the applicability of the present method on real samples, a TLC isolated PG fraction of lipids extracted from *M. capsulatus* was analyzed. It is reported that the PL and FA content is dependent on the growth conditions [33], but this was not a topic of the present study. Figure 8a shows the negative ESI/MS scanning recorded spectrum of the PG fraction, and a major ion at *m/z* 719 is observed in addition to the minor ions at *m/z* 688, 689, and 721. The product-ion spectrum of *m/z* 719 recorded at E_{Lab} 30 eV is displayed in Figure 8b. The ions at *m/z* 253 (100%) and 255 (35%) indicate that the FAs 16:1 and 16:0, respectively, are components of this PL species. The observed ions at *m/z* 483, 481, 465, and 463, which correspond to $[M - H - R'_2CH{=}C{=}O]^-$, $[M - H - R'_1CH{=}C{=}O]^-$, $[M - H - R_2COOH]^-$, and $[M - H - R_1COOH]^-$, respectively, support this. Further, a loss of 74 u from the ions at *m/z* 465 and 463 results in the $[M - H - 74 - R_2COOH]^-$ and $[M - H - 74 - R_1COOH]^-$ ions at *m/z* 391 and 389, respectively. The observed ions and the ratios between the ion-pairs are all consistent with the presence of a 16:0/16:1Δ^x PG species.

The sample was then subjected to a derivatisation by OsO_4 and the resulting negative ESI/MS recorded scan is shown in Figure 8c. The major ion of this spectrum is the ion at *m/z* 753. The product-ion spectrum of the *m/z* 753 ion recorded at E_{Lab} 65 eV is displayed in Figure 8d. The ion at *m/z* 287 corresponds to the (n,n + 1)-$(OH)_2$-16:0 carboxylate and this ion undergoes further fragmentations that reveal information on the positions of the hydroxyl groups. Thus, the ions at *m/z* 201, 171, 143, and 113 suggest the presence of a 9,10-$(OH)_2$-16:0 FA whereas the less abundant ions at *m/z* 215, 185, 129 and 99 suggest the presence of a 10,11-$(OH)_2$-16:0 FA.

To support the presence of 9,10-$(OH)_2$-18:0 in the PG species, a CAD product-ion spectrum of deprotonated 9,10-$(OH)_2$-16:0 was recorded (E_{Lab} 28 eV). This is shown in Figure 8e. The ions at *m/z* 201, 171, 143, and 113 are of high abundance in Figure 8e, whereas the ions proposed to be formed from 10,11-$(OH)_2$-16:0 are absent or low abundant.

The GC/MS analysis of the DMOX derivatives

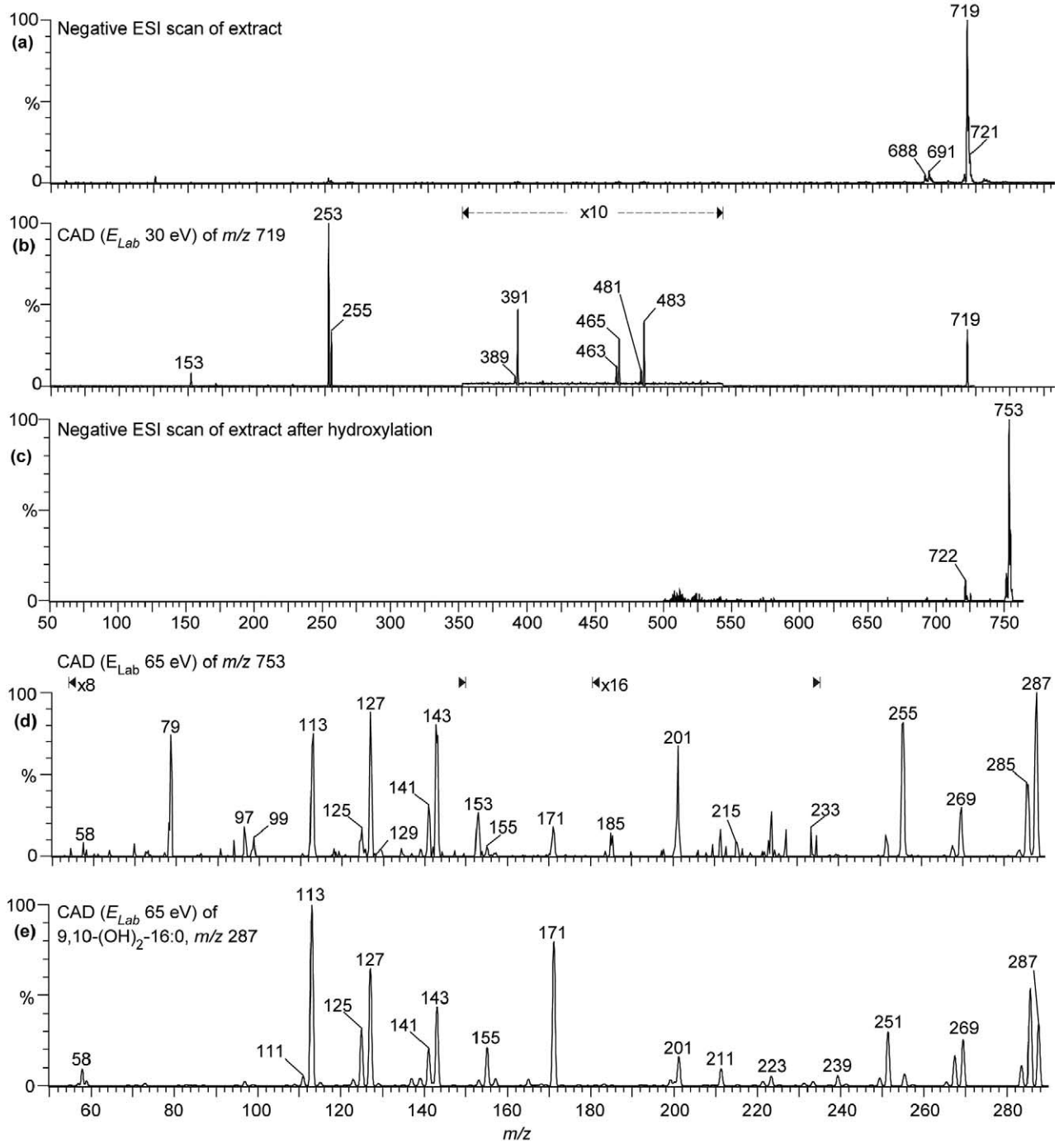

Figure 8. (**a**) Negative ESI scanning of the infused *M. capsulatus* extract. (**b**) The product-ion spectrum of *m/z* 719 (E_{Lab} 30 eV), (**c**) negative ESI scanning of the infused *M. capsulatus* extract after derivatization, (**d**) the product-ion spectrum of *m/z* 753 (E_{Lab} 65 eV), and (**e**) the product-ion spectrum of 9,10-$(OH)_2$-16:0, *m/z* 287, recorded at E_{Lab} 28 eV. In (**d**) and (**e**) only the range *m/z* 50–290 is displayed.

showed that the sample consisted primarily of the FAs 16:1Δ^9 (retention time; t_R = 36.15, area: 1,100,000) and 16:1Δ^{10} (t_R = 36.30, area: 200,000) in addition to a minor amount of 16:1Δ^{11} (t_R = 36.50, area: 9,500). The DMOX derivatives of 16:1 gave molecular ions ($M^{+\cdot}$) at *m/z* 307. A gap of 12 u between two ions, which are of lower abundance than the adjacent ions, allows the assignment of a double bond in an EI mass spectrum of a DMOX-FA derivative [17]. For 16:1Δ^9, the double bond was identified by the ions at *m/z* 196 (25%) and 208 (20%). These ions were surrounded by *m/z* 182 (70%), 222 (30%) and 236 (60%). For 16:1Δ^{10}, the double bond was identified by the ions at *m/z* 210 and 222, whereas the analogous ions occurred at *m/z* 224 and 236 for

16:1Δ^{11}. The latter isomer was not observed in the CAD product-ion spectrum of *m/z* 753. Thus, a chromatographic separation of the species prior to analysis by negative ESI-MS/MS may be beneficial in order to detect all the isobaric species of the sample. However, the ratio of the areas of 16:1Δ^{10} and 16:1Δ^{9} (GC/MS; 1:5.5) is comparable with the intensity ratio of *m/z* 185 from 10,11-$(OH)_2$-16:0 and *m/z* 171 from 9,10-$(OH)_2$-16:0 (ESI-MS/MS; 1:7). In conclusion, the sample from *M. capsulatus* consisted mainly of 16:0/16:1Δ^{9} PG and 16:0/16:1Δ^{10} PG, in addition to a minute amount of 16:0/16:1Δ^{11} PG.

Discussions

Product-Ion Abundance

The product-ions indicating the hydroxyl group positions in PA and PS species are of lower abundance than those from PG. This is recognized in the CAD product-ion spectra of 16:0/11,12-$(OH)_2$-18:0 PA and 16:0/11,12-$(OH)_2$-18:0 PG (Figures 2d and 6g, respectively) and 16:0/6,7-$(OH)_2$-18:0 PS and 16:0/6,7-$(OH)_2$-18:0 PG (Figures 4b and 6e, respectively). This is probably due to the preferred formation of the *sn*-1 carboxylate for PA [1–4] and PS [1, 3, 4, 8, 10], whereas *sn*-2 carboxylates are preferred for PG [1, 3, 5–7].

The CAD product-ion spectrum of the 6,7-$(OH)_2$-18:0 carboxylate is different from the other derivatized mono-unsaturated FAs as the product-ions resulting from Pathways **1a** and **1b** in Scheme **1** are both of low abundance. The proximity to the charged site could be one reason for this, i.e., proton transfer by Pathway **1c** and **1d** (Scheme **1**) is more likely to occur.

E_{Lab}

The PL species discussed above were fully characterized by utilizing a different E_{Lab} in the two CAD experiments: E_{Lab} 30 eV for the native species and E_{Lab} 60 eV (or 65 eV) for the vicinally di-hydroxylated species. The intensity-ratios of certain product-ions in the CAD product-ion spectra of the native PLs are useful for assignment of FA regioisomerism. From the CAD product-ion spectra (E_{Lab} 30 eV) of the deprotonated 1,2-di-hydroxylated PL species it was observed that some of these ratios fluctuated around one, probably due to further fragmentation of the derivatizd FA. Thus, these ratios are not useful for regioisomeric assignments in the derivatizd PLs. These results are not included in this work, except for 16:0/11,12-$(OH)_2$-18:0 PA (Figure 2b). Because of this it is more appropriate to analyze the native species rather than the derivatives at E_{Lab} 30 eV prior to the E_{Lab} 60 eV (65 eV) analysis of the derivatives. The latter condition provides information on hydroxyl group positions and hence the double bonds of the native FAs.

Fragmentation

The derivatized FAs are more prone to undergo charge-driven reactions as the number of hydroxyl groups increases. This may be explained by the feasible formation of intra-molecular hydrogen-bonds. A mass spectrum is a result of a number of competitive and consecutive reactions, which may explain why few of the ion-series produced by the mechanisms of Scheme **2** (*m/z* values are summarized in Table 2) are complete. Pathway **2b** is preferred for cleavage of the bonds adjacent to the most distal hydroxyl groups along with Pathway **1c** and **1d** (Scheme **1**). The product-ions resulting from Pathway **1a** and **1b** (Scheme **1**) are preferred to the proposed Pathways **2a–2c** in Scheme **2** only for the cleavage of the bonds adjacent to the two proximal hydroxyl groups (x = 0).

The present method is less sensitive for PLs than for free FAs (with respect to product-ion abundance), as some additional important ions are observed in the spectra of the derivatized free FAs [17]. One explanation to this is that a higher E_{Lab} must be applied in the analysis of PLs. This will probably result in increased ion-beam divergence and sample loss in the collision cell.

Conclusions

ESI-MS/MS analysis of native acidic PL species by their deprotonated molecules reveals all structural features of the species except for the location of olefinic sites. By converting the double bonds to their vicinally di-hydroxylated derivatives, the positions of the hydroxyl groups and hence the positions of the double bond(s) of the native FAs are revealed by a second ESI-MS/MS experiment on the deprotonated molecule. The results of the present study have demonstrated the usefulness of vicinal di-hydroxylation of unsaturated FAs in order to achieve a complete structural elucidation of PLs by ESI low-energy MS/MS. It has also been shown that isobaric species constituting isomeric FAs are distinguished, which even applies for mixtures. The spectra of deprotonated vicinally di-hydroxylated FAs originally containing more than three double bonds yielded very complicated and difficultly interpretable spectra upon CAD. For this reason PL species constituting such FAs were not included in the study. Anyhow, for PL species constituting FAs with a low degree of unsaturation, the present method should provide lipid chemists a powerful tool whereby acidic PLs are fully characterized.

Acknowledgments

This project was financially supported by the Norwegian Research Council (grant no. 128256/420). The authors are deeply indebted to Dr. Elena L. Vodovozova, at Shemyakin and Ovchinnikov Institute of Bioorganic Chemistry, Russian Academy of Sciences, Moscow, Russia, for invaluable hints and suggestions regarding the synthesis of PC from 2-lysophosphatidylcholine, Dr. Hanne Müller and Dr. Anders Skrede at the Norwegian University for

Agricultural Sciences, Ås, Norway, for providing them with the *M. capsulatus* samples, Dr. Hans Grav, University of Oslo, Norway, for teaching them the beneficial oxazoline analysis.

References

1. Fang, J. S.; Barcelona, M. J. Structural Determination and Quantitative Analysis of Bacterial Phospholipids Using Liquid Chromatography Electrospray Ionization Mass Spectrometry. *J. Microbiol. Methods* **1998,** *33*, 23–35.
2. Hsu, F. F.; Turk, J. Charge-Driven Fragmentation Processes in Diacyl Glycerophosphatidic Acids Upon Low-Energy Collisional Activation. A Mechanistic Proposal. *J. Am. Soc. Mass Spectrom.* **2000,** *11*, 797–803.
3. Smith, P. B. W.; Snyder, A. P.; Hatden, C. S. Characterization of Bacterial Phospholipids by Electrospray Ionization Tandem Mass Spectrometry. *Anal. Chem.* **1995,** *67*, 1824–1830.
4. Hvattum, E.; Hagelin, G.; Larsen, A. Study of Mechanisms Involved in the Collision-Induced Dissociation of Carboxylate Anions from Glycerophospholipids Using Negative Ion Electrospray Tandem Quadrupole Mass Spectrometry. *Rapid Commun. Mass Spectrom.* **1998,** *12*, 1405–1409.
5. Han, X. L.; Gross, R. W. Electrospray-Ionization Mass Spectroscopic Analysis of Human Erythrocyte Plasma-Membrane Phospholipids. *Proc. Nat. Acad. Sci. U.S.A.* **1994,** *91*, 10635–10639.
6. Karlsson, A. A.; Michelsen, P.; Larsen, A.; Odham, G. Normal-Phase Liquid Chromatography Class Separation and Species Determination of Phospholipids Utilizing Electrospray Mass Spectrometry Tandem Mass Spectrometry. *Rapid Commun. Mass Spectrom.* **1996,** *10*, 775–780.
7. Hsu, F. F.; Turk, J. Studies on Phosphatidylglycerol with Triple Quadrupole Tandem Mass Spectrometry with Electrospray Ionization: Fragmentation Processes and Structural Characterization. *J. Am. Soc. Mass Spectrom.* **2001,** *12*, 1036–1043.
8. Kerwin, J. L.; Tuininga, A. R.; Ericsson, L. H. Identification of Molecular Species of Glycerophospholipids and Sphingomyelin Using Electrospray Mass Spectrometry. *J. Lipid Res.* **1994,** *35*, 1102–1114.
9. Hsu, F. F.; Turk, J. Characterization of Phosphatidylinositol, Phosphatidylinositol-4-Phosphate, and Phosphatidylinositol-4,5-Bisphosphate by Electrospray Ionization Tandem Mass Spectrometry: A Mechanistic Study. *J. Am. Soc. Mass Spectrom.* **2000,** *11*, 986–999.
10. Brügger, B.; Erben, G.; Sandhoff, R.; Wieland, F. T.; Lehmann, W. D. Quantitative Analysis of Biological Membrane Lipids at the Low Picomole Level by Nano-Electrospray Ionization Tandem Mass Spectrometry. *Proc. Nat. Acad. Sci. U.S.A.* **1997,** *94*, 2339–2344.
11. Bryant, D. K.; Orlando, R. Location of Unsaturated Positions in Phosphatidyl Cholines by Consecutive-Reaction Monitoring. *Rapid Commun. Mass Spectrom.* **1991,** *5*, 124–127.
12. Jensen, N. J.; Tomer, K. B.; Gross, M. L. Fast Atom Bombardment and Tandem Mass Spectrometry of Phosphatidylserine and Phosphatidylcholine. *Lipids* **1986,** *21*, 580–588.
13. Jensen, N. J.; Tomer, K. B.; Gross, M. L. Fast Atom Bombardment MS/MS for Phosphatidylinositol, -Glycerol, -Ethanolamine, and Other Complex Phospholipids. *Lipids* **1987,** *22*, 480–489.
14. Harrison, K. A.; Murphy, R. C. Direct Mass Spectrometric Analysis of Ozonides: Application to Unsaturated Glycerophosphocholine Lipids. *Anal. Chem.* **1996,** *68*, 3224–3230.
15. Dupau, P.; Epple, R.; Thomas, A. A.; Fokin, V. V.; Sharpless, K. B. Osmium-Catalyzed Dihydroxylation of Olefins in Acidic Media: Old Process, New Tricks. *Adv. Synth. Cat.* **2002,** *344*, 421–433.
16. McCloskey, J.; McClelland, M. Mass Spectra of O-Isopropylidene Derivatives of Unsaturated Fatty Esters. *J. Am. Chem. Soc.* **1965,** *87*, 5090–5093.
17. Moe, M. K.; Jensen, E. Structure Elucidation of Unsaturated Fatty Acids after Vicinal Hydroxylation of the Double Bonds by Negative Electrospray Ionisation Low-Energy Tandem Mass Spectrometry. *Eur. J. Mass Spectrom.* **2004,** *10*, 47–55.
18. Moe, M. K.; Anderssen, T.; Strøm, M. B.; Jensen, E. Vicinal Hydroxylation of Unsaturated Fatty Acids for Structural Characterization of Intact Neutral Phospholipids by Negative Electrospray Ionization Tandem Quadrupole Mass Spectrometry. *Rapid Commun. Mass Spectrom.* **2004,** *18*, 2121–2130.
19. Vodovozova, E. L.; Molotkovsky, J. G. A Novel Catalyst for O-Acylation in Lipid Chemistry. *Tetrahedron Lett.* **1994,** *35*, 1933–1936.
20. Vodovozova, E. L.; Molotkovsky, J. G. A Novel Catalyst for O-Acylation in Lipid Chemistry. *Tetrahedron Lett.* **1994,** *35*, 8062.
21. Onyango, A. N.; Inoue, T.; Nakajima, S.; Baba, N.; Kaneko, T.; Matsuo, M.; Shimizu, S. Synthesis and Stability of Phosphatidylcholines Bearing Polyenoic Acid Hydroperoxides at the *Sn*-2 Position. *Angew. Chem. Int. Ed.* **2001,** *40*, 1755–1757.
22. Baba, N.; Aoishi, A.; Shigeta, Y.; Nakajima, S.; Kaneko, T.; Matsuo, M.; Shimizu, S. Chemoenzymic Synthesis of Phosphatidyl-L-Serine Hydroperoxide. *Biosci. Biotechnol. Biochem.* **1994,** *58*, 1927–1928.
23. Yoneda, K.; Sasakura, K.; Tahara, S.; Iwasa, J.; Baba, N.; Kaneko, T.; Matsuo, M. Chemoenzymatische Synthese Optisch Aktiver Hydroperoxide von Phosphatidylglycerin und -Ethanolamin mit Lipase, Lipoxygenase und Phospholipase D. *Angew. Chem* **1992,** *104*, 1386–1387.
24. Mandal, S. B.; Sen, P. C.; Chakrabarti, P. In Vitro Synthesis of Phosphatidylinositol and Phosphatidylcholine by Phospholipase D. *Phytochemistry* **1980,** *19*, 1661–1663.
25. Servi, S. Phospholipases as Synthetic Catalysts. *Topics Curr. Chem.* **1999,** *200*, 127–158.
26. Folch, J.; Lees, M.; Sloane Stanley, G. H. A Simple Method for the Isolation and Purification of Total Lipides from Animal Tissues. *J. Biol. Chem.* **1957,** *226*, 497–509.
27. Bligh, E. G.; Dyer, W. J. A Rapid Method of Total Lipid Extraction and Purification. *Can. J. Biochem. Physiol.* **1959,** *37*, 911–917.
28. Lewis, T.; Nichols, P. D.; McMeekin, T. A. Evaluation of Extraction Methods for Recovery of Fatty Acids from Lipid-Producing Microheterotrophs. *J. Microbiol. Methods* **2000,** *43*, 107–116.
29. Touchstone, J. C.; Levin, S. S.; Dobbins, M. F.; Matthews, L.; Beers, P. C.; Gabbe, S. G. (3-*Sn*-Phosphatidyl) Cholines (Lecithins) in Amniotic Fluid. *Clin. Chem.* **1983,** *29*, 1951–1954.
30. Safonova, E. F.; Nazarova, A. A.; Selemenev, V. F.; Brezhneva, T. A.; Slivkin, A. I. Selecting Optimum Parameters for the TLC Separation of Phospholipids. *Pharmaceut. Chem. J.* **2002,** *36*, 206–208.
31. Fried, B., Lipids. In *Handbook of Thin Layer Chromatography*; Fried, B.; Sherma, J., Eds.; Marcel Dekker: New York, 1991; pp 593–622.
32. Garrido, J. L.; Medina, I. One-Step Conversion of Fatty-Acids into Their 2-Alkenyl-4,4-Dimethyloxazoline Derivatives Directly from Total Lipids. *J. Chromatogr. A* **1994,** *673*, 101–105.
33. Spitzer, V. Structure Analysis of Fatty Acids by Gas Chromatography Low Resolution Electron Impact Mass Spectrometry of Their 4,4-Dimethyloxazoline Derivatives—a Review. *Prog. Lipid Res.* **1996,** *35*, 387–408.
34. Kerwin, J. L.; Wiens, A. M.; Ericsson, L. H. Identification of Fatty Acids by Electrospray Mass Spectrometry and Tandem Mass Spectrometry. *J. Mass Spectrom.* **1996,** *31*, 184–192.
35. Moe, M. K.; Strøm, M. B.; Jensen, E.; Claeys, M. Negative Electrospray Ionization Low-Energy Tandem Mass Spectrometry of Hydroxylated Fatty Acids. A Mechanistic Study. *Rapid Commun. Mass Spectrom.* **2004,** *18*, 1731–1740.